# Heavy-ion-induced desorption yields of cryogenic surfaces bombarded with 1.4 MeV/u xenon ions

Donat Philipp Holzer[*] and Edgar Mahner

*CERN, 1211 Geneva 23, Switzerland*

Holger Kollmus, Markus Bender, Daniel Severin, and Marc Wengenroth

*GSI, 64291 Darmstadt, Germany*

Heavy-ion-induced desorption of two different cryogenic targets was studied with a new experimental setup installed at the GSI High Charge State Injector. One gold-coated and one amorphous-carbon-coated copper target, bombarded under perpendicular impact with 1.4 MeV/u $Xe^{18+}$ ions, were tested. Partial pressure rises of $H_2$, CO, $CO_2$, and $CH_4$ and effective desorption yields were measured at 300, 77, and 8 K using continuous heavy-ion bombardment. We found that the desorption yields decrease with decreasing target temperature and measured the yield rises as a function of CO gas cryosorbed at 8 K. In this paper we describe the experimental system comprising a new cryogenic target assembly, the preparation of the targets, the test procedure, and the evaluation of the effective pumping speed of the setup. Pressure rise and gas adsorption experiments are described; the obtained results are discussed and compared with literature data.

## I. INTRODUCTION

Heavy-ion-induced molecular desorption can be a serious limitation for synchrotrons operating with low charge-state heavy ions due to the observed large pressure rises that often reduce the obtainable beam intensity and lifetime of the accelerator [1]. Since 2000, several laboratories have studied this phenomenon [1–3] to find appropriate mitigation methods. So far, most of the experiments investigated a variety of ambient temperature targets, which were bombarded with heavy ions to measure their desorption yields. First experiments with cryogenic targets were performed at CERN; accelerator relevant materials as bare and gold-coated copper targets were used there [4,5].

Desorption yield measurements at cryogenic temperatures are motivated by the design of future heavy-ion accelerators, for example, SIS100, which is part of the GSI FAIR (Facility for Antiproton and Ion Research) project [6], and the operation of the Large Hadron Collider (LHC). Two different targets were chosen for our studies at HLI; the first material is gold-coated copper, which has already been investigated at ambient and cryogenic temperatures [5,7]. Such gold coatings are of special interest because they are part of the baseline design for the SIS100 cryocatcher [8]. As a second target an amorphous

carbon thin film, sputter coated onto a copper substrate, was chosen. The dynamic vacuum properties of such films are important to investigate since amorphous carbon coatings are foreseen to mitigate the electron cloud effect [9] in the CERN Super Proton Synchrotron [10]. Ambient temperature desorption yield measurements were reported recently [11].

## II. EXPERIMENT

### A. Experimental setup

The accelerator providing the ion beam for this experiment is the GSI High Charge State Injector (HLI). The HLI is capable of delivering ions at a fixed energy of 1.4 MeV/u, with pulse lengths between 0.49 and 5.5 ms at a repetition rate between 0.1 and 50 Hz. The accelerator is described in detail elsewhere [12]. The experimental layout is shown in Fig. 1.

A gate valve separates the HLI from the experimental setup such that samples can be changed without disturbing accelerator operation. Downstream the gate valve, adjustable beam collimators are installed to control the beam size. The collimator jaws are electrically isolated and can be used to measure the beam current. To separate the desorption experiment from the high pressure ($10^{-7}$ mbar) of the HLI, a differential pumping system comprising two separate vacuum chambers are installed between the collimators and the sample chamber (see Fig. 1).

The first vacuum chamber contains a turbo molecular pumping (TMP) group and a baffle, which is cooled to liquid nitrogen temperature. The cold baffle retains hydrocarbons and water vapor originated from the linac.

---

[*]Also at Vienna University of Technology, Vienna, Austria. donat.philipp.holzer@cern.ch
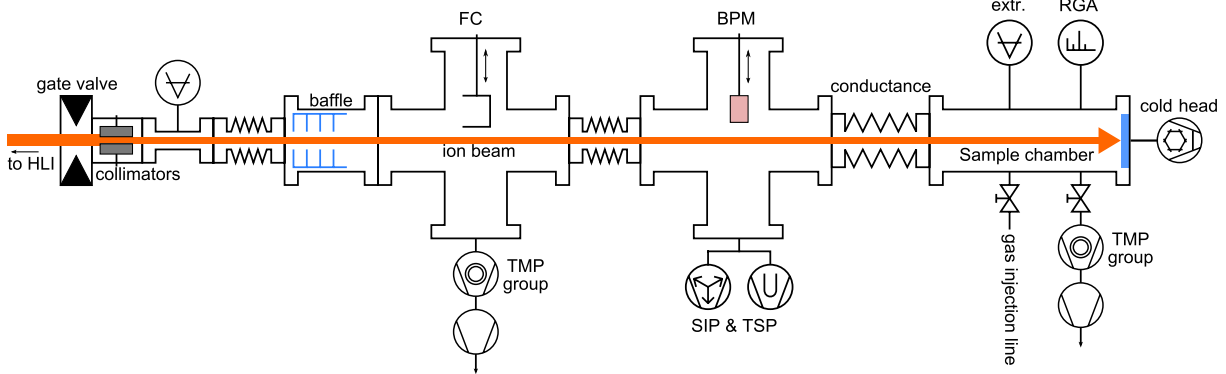
FIG. 1. Schematic view of the experimental setup, which has been attached at the GSI HLI for heavy-ion-induced desorption measurements at 1.4 MeV/u.

A retractable Faraday cup is installed and used to measure the beam current.

The second vacuum chamber is equipped with a sputter ion pump (SIP) and an integrated titanium sublimation pump (TSP) providing a total pumping speed of about 1000 l/s for nitrogen. It also houses a retractable Chromolux (Cr doped $Al_2O_3$) beam position monitor, which is used to align the beam.

At the end of the experimental line, the installed sample chamber is equipped with another TMP group, which is used during pump-down and bakeout of the entire setup. The group is separated from the setup (valve closed) during heavy-ion desorption experiments. Pumping is provided through a conductance (ø = 63 mm, l = 228 mm) resulting in an effective pumping speed of about 82 l/s ($N_2$ equivalent). A gas injection system is also connected to the sample chamber. It comprises a variable leak valve and a membrane pump.

For desorption experiments at cryogenic temperatures a dedicated cold-head assembly was designed, built, and installed at the end of the experimental setup (see Fig. 2).

The target used for heavy-ion-induced desorption measurements is mounted on a dedicated sample holder, which is attached to the second stage of the cold head (Leybold Coolpower 7/25). It is equipped with two temperature sensors (LakeShore diode DT 470-CU-12A). One diode is mounted on the backside of the test sample, the second one is connected onto the copper radiation shield of the cold-head assembly. In order to control the sample temperature, the target holder is equipped with a resistive DC heater, which provides a maximum heating power of 62.5 W. Using this setup, the sample temperature during the experiments, with impinging beam, was found to be stable within 0.3 K or better.

For partial and total pressure measurements, the sample vacuum chamber is equipped with a Balzers QMA 125 residual gas analyzer (RGA) and a calibrated Leybold IE 514 extractor gauge (extr.). The RGA was calibrated *in situ* with respect to the total pressure gauge.

## B. Fabrication and preparation of targets

Fabrication, cleaning, and coating of the tested samples were performed at CERN. Two discs were machined from oxygen-free electronic grade copper with a thickness of 7 mm and a diameter of 50 mm. After standard cleaning,
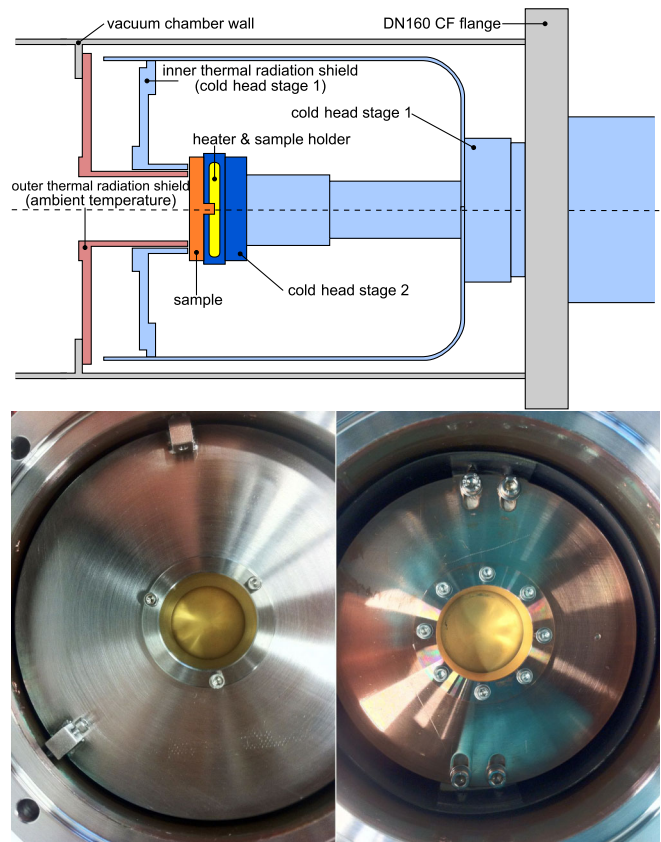


FIG. 2. Top: schematic view of the cold-head assembly used for heavy-ion-induced desorption measurements at cryogenic temperatures. Bottom left: frontal view of the cold head with installed gold-coated target and inner thermal radiation shield, thermally anchored at the first stage of the cold head. Bottom right: installed target and outer thermal radiation shield anchored at ambient temperature.

one of the targets was coated with amorphous carbon by magnetron sputtering. The used deposition system, the sputtering parameters, and resulting sample topography are described in detail elsewhere [11,13]. The film thickness was measured by scanning electron microscopy to be 360 nm. The second copper target was galvanically coated with a 7 $\mu$m thin gold film and a 2 $\mu$m thin nickel underlayer acting as a diffusion barrier during bakeout of the experimental setup. This target was gold coated simultaneously with another copper sample, which was previously tested for low-temperature heavy-ion-induced desorption at LINAC 3 [5].

### C. Experimental procedure

After sample installation and pump-down of the experimental line, the setup was baked at 150 °C for 48 hours. Heavy-ion-induced desorption yields were measured at a fixed projectile impact angle of $\theta = 0°$ (perpendicular impact). The HLI beam consisted of $Xe^{18+}$ ions with an energy of 1.4 MeV/u, a pulse length of 3.18 ms, and a repetition rate of 4.8 Hz. Both targets were bombarded with an average ion flux of $2 \times 10^9$ ions per second. Prior to each individual desorption experiment, the Faraday cup was used to measure the beam current from which the ion flux is calculated. The collimator current measurements allowed continuous monitoring of the beam current. The collimator jaws were adjusted to result in a beam spot size of $1 \times 1$ cm$^2$ on the target. As described above, the amorphous-carbon-coated copper target (aC/Cu sample) and the gold-coated copper target (Au/Cu sample) were tested for desorption at 300, 77, and 8 K.

The pressure rise method [14] was used to determine the yields of the studied samples. The effective heavy-ion-induced desorption yield $\eta_{\text{eff}}$ is calculated as

$$\eta_{\text{eff}} = \frac{\Delta P S}{\dot{N}_{Xe} k_b T}, \tag{1}$$

where $\Delta P$ is the total pressure increase, $S$ is the effective pumping speed, $\dot{N}_{Xe}$ is the average number of impacting $Xe$ ions per second, $k_b$ is the Boltzmann constant, and $T$ is the temperature of the released gas at the position of the pressure gauge (300 K). $\Delta P \times S$ is defined as the gas flux $Q_0$, which in this case is the gas flux of desorbed gas molecules produced by the impinging ions on a target.

### D. Pumping speed of cryogenic targets

Since the cold head acts as a cryopump at cryogenic temperatures, the effective total pumping speed $S$ increases when the target is cooled down. We define

$$S = S_{\text{eff}} + S_{\text{cryo}}(\sigma), \tag{2}$$

where $S_{\text{eff}}$ is the ambient temperature effective pumping speed of the TSP and SIP in the experimental chamber and $S_{\text{cryo}}$ is the effective pumping speed generated by the cold
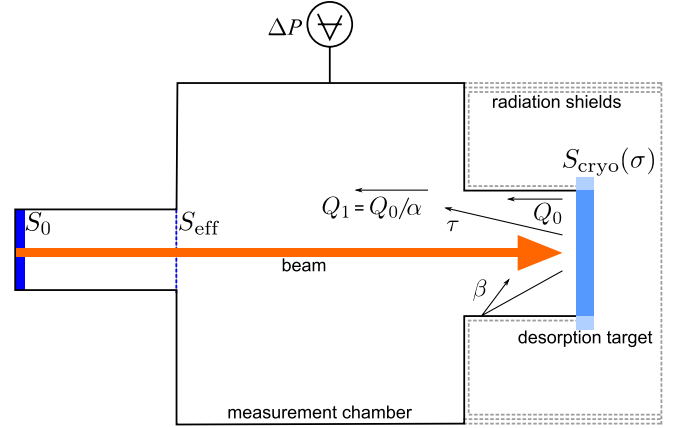


FIG. 3. Schematic display of the gas flux, pumping speeds, and geometry relevant for the heavy-ion-induced desorption of a cryogenic target installed in the experimental vacuum chamber.

surface of the target, which depends on the sticking probability $\sigma$.

At this point we want to underline that in our previous heavy-ion-induced desorption experiment of cryogenic targets at CERN-LINAC 3 [5], the so-called single-shot technique [14] was used to determine $S_{\text{cryo}}$. Unfortunately this was not possible for the GSI-HLI study presented here. In order to quantify the influence of cryopumping in our system we have chosen Monte Carlo simulations as well as analytical calculations, which are described next.

The gas flux $Q_0$, generated by the ion-induced desorption at the target, is reduced by a factor $\alpha$ that depends on the target sticking probability $\sigma$.

The radiation shield of the cold-head assembly, as schematically shown in Fig. 3, forms a short cylindrical duct in front of the target introducing a certain transmission probability $\tau$ and backscattering probability $\beta = 1 - \tau$ for released gas molecules.

The gas flux arriving in the measurement vacuum chamber, $Q_1$, is therefore equal to $Q_0$ times the fraction of gas that is not backscattered and pumped by the target. We find

$$Q_1(\sigma) = Q_0[\tau + \beta(1 - \sigma)\tau + \beta^2(1 - \sigma)^2\tau + \ldots] \tag{3}$$

$$= Q_0\tau \sum_{n=0}^{\infty} \beta^n (1 - \sigma)^n \tag{4}$$

$$= Q_0\tau\left(\frac{1}{1 - \beta(1 - \sigma)}\right). \tag{5}$$

Therefore, the reduction factor $\alpha$ is defined as

$$\alpha(\sigma) = \frac{1 - \beta(1 - \sigma)}{\tau} \tag{6}$$

and finally $Q_0$ can be calculated as

$$Q_0(\sigma) = Q_1\alpha(\sigma) \tag{7}$$
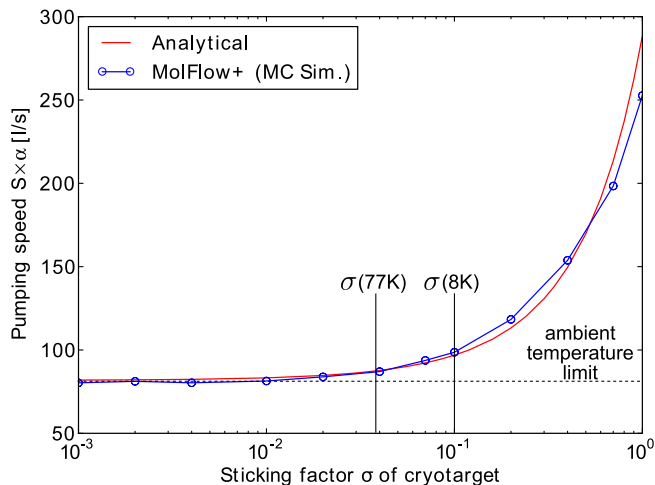
$$= \Delta P S \alpha(\sigma). \tag{8}$$

FIG. 4. Product of pumping speed $S$ and reduction factor $\alpha$ as a function of sticking probability $\sigma$ for the used experimental setup calculated; the shown curves were calculated for CO.

We have calculated the product of the pumping speed $S$ and the reduction factor $\alpha$ as a function of the sticking probability $\sigma$. For the specific geometry of our experimental setup with $S_0 = 1000$ l/s for CO, we find $\tau = 0.582$ and $\beta = 0.418$ [15]. In addition, the measurement setup has been simulated using the Monte Carlo flow analysis software MolFlow+ [16]. The obtained results are shown in Fig. 4.

We find that the analytical calculation is in good agreement with the Monte Carlo simulation (see Fig. 4). A slight difference is only observed for $\sigma$ values close to 1. This result was expected, since the Monte Carlo simulation takes into account that the relevant desorbing surface is only the beam spot in the middle of the target, and not the entire surface, which is the implicit assumption in the analytical case. Because the calculation of the effective desorption yields $\eta_{\text{eff}}$, the values from the Monte Carlo simulation were used in this work.

So far we have derived a relation for $S \times \alpha$ as a function of the sticking probability $\sigma$. In the following we will determine the sticking probability at the required temperatures of 77 and 8 K.

We used the measured pumping speeds $S_{\text{cryo}}$ of our previous LINAC 3 heavy-ion-induced desorption studies [5] to obtain $\sigma(77 \text{ K})$ and $\sigma(8 \text{ K})$. This approach is well justified because the bombarded target surfaces (Au/Cu, aC/Cu) and the target temperatures (300, 77, 8 K) were identical with the LINAC 3 experiment. Under such conditions the sticking probabilities $\sigma$, which are independent of the sample size and the experimental setup, can be derived from our previous experiment. We used the relation

$$\sigma = \frac{S_{\text{max}}}{S_{\text{cryo}}} = \frac{A k_a}{S_{\text{cryo}}}, \tag{9}$$

where $S_{\text{max}}$ is the maximum possible pumping speed of a given surface, $A$ is the surface area, and $k_a$ is the incident volume per area per unit time, directly related to the average speed $v_a$ of molecules, $k_a = \frac{1}{4} v_a$.

## III. RESULTS

### A. Desorption yield measurements at 300 K

The gold-coated copper and amorphous-carbon-coated targets were continuously bombarded for 15 min with 1.4 MeV/u $Xe^{18+}$ ions impacting under perpendicular incidence. Total and partial pressure rises were measured with the extractor gauge and the residual gas analyzer. The obtained results are shown in Fig. 5.

For the aC/Cu sample it has to be noted that about 600 s after the start of the continuous heavy-ion bombardment, the RGA was switched to scan mode to acquire a full mass
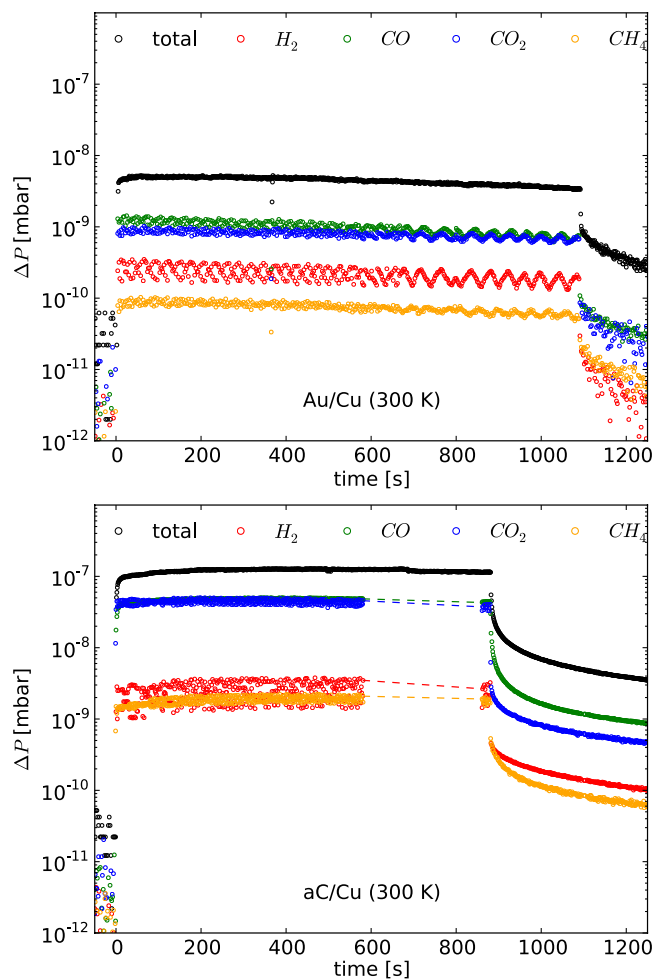


FIG. 5. Heavy-ion-induced pressure rises at 300 K target temperature. Partial pressure rises ($\Delta P$) of $H_2$, CO, $CO_2$, $CH_4$, and total pressure rises measured for the Au/Cu and aC/Cu samples continuously bombarded under $\theta = 0°$ with 1.4 MeV/u $Xe^{18+}$ ions are shown.

spectrum. Therefore, no time-dependent data points are available for about 200 s (see Fig. 5).

For both targets the heavy-ion-induced desorption at 300 K is dominated by CO and $CO_2$. Compared to $H_2$, the CO and $CO_2$ partial pressure increase is a factor of 3 higher for the Au/Cu sample and more than 1 order of magnitude higher for the aC/Cu sample.

Using the pumping speed relation shown in Fig. 4 and assuming a sticking probability of $\sigma$ below 0.01, the effective desorption yields were calculated from the total pressure rises. We find $\eta_{eff} \approx 5400$ molecules/ion for Au/Cu and $\eta_{eff} \approx 127000$ molecules/ion for aC/Cu.

The relative error of the calculated desorption yields is dominated from uncertainties in the pressure measurements and is estimated to $\pm 30\%$. An additional variation of the desorption yield, even for a similar target material, cannot be excluded due to the potential influence of surface treatment, cleaning, storage, and bakeout. This variation has not been taken into account in this analysis, and therefore the given values are called *effective* desorption yields.

### B. Desorption yield measurements at 77 K

After the desorption measurements at ambient target temperature, each sample was cooled down from 300 to 77 K where the temperature was stabilized using the control system comprising the DC heater and the temperature sensors attached to the samples.

The measured pressure rises at 77 K are compared in Fig. 6. For Au/Cu, the partial pressures of $H_2$, CO, and $CO_2$ contribute roughly equal to the pressure rise. $H_2$ is now the dominating measured gas for aC/Cu. The hydrogen partial pressure is more than a factor of 10 higher than for CO and $CO_2$.

At 77 K we obtain for a sticking probability of $\sigma \approx 0.037$ the following heavy-ion-induced desorption yields: $\eta_{eff} \approx 620$ molecules/ion (Au/Cu) and $\eta_{eff} \approx 3100$ molecules/ion (aC/Cu).

### C. Desorption yield measurements at 8 K

Following the desorption experiments at 77 K, both samples were further cooled down to 8 K, which is the limit temperature that could be reached in this measurement setup.

The straight line visible in Fig. 7 for the aC/Cu sample is an artefact, most probably introduced by the electronics of the total pressure gauge. To some extent, the same artefact is also visible in Fig. 6 for the Au/Cu target. The erroneous data points were not taken into account for the desorption yield evaluation.

The measured pressure rises at 8 K are compared in Fig. 7. With a sticking probability of $\sigma \approx 0.1$ the resulting effective desorption yields are $\eta_{eff} \approx 430$ molecules/ion for Au/Cu and $\eta_{eff} \approx 1000$ molecules/ion for aC/Cu.



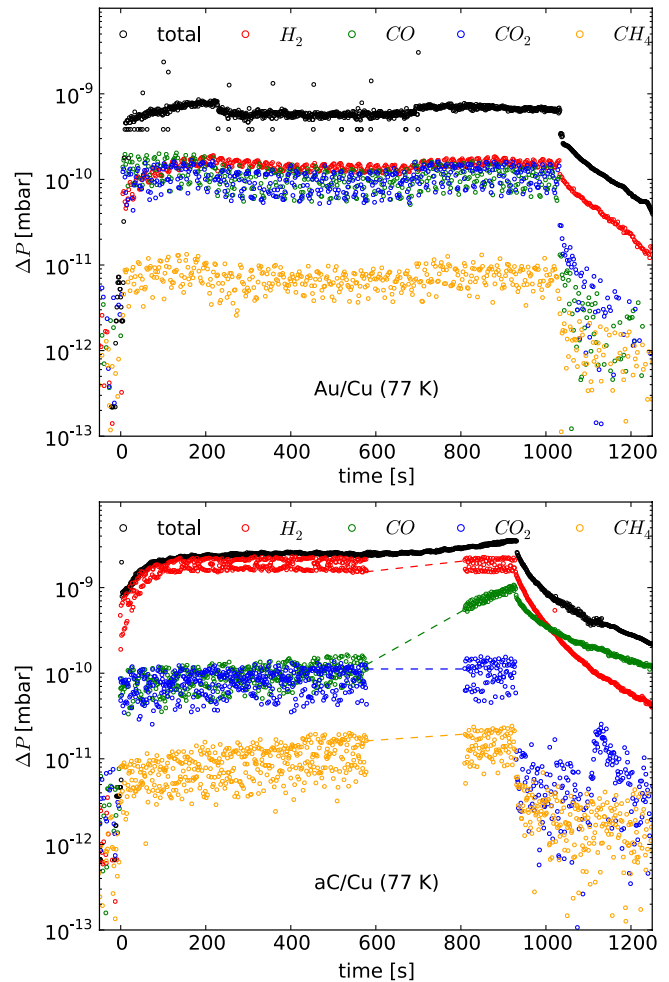FIG. 6.   Heavy-ion-induced pressure rises at 77 K target temperature. Partial pressure rises ($\Delta P$) of $H_2$, CO, $CO_2$, $CH_4$, and total pressure rises measured for the Au/Cu and aC/Cu samples continuously bombarded under $\theta = 0°$ with 1.4 MeV/u $Xe^{18+}$ ions are shown.

### D. Desorption yields for different gas species

A comparison of the effective desorption yields $\eta_{eff}$, calculated from the total and partial pressures, is shown in Table I and II.

The data from total and partial pressure measurements are in reasonable agreement for both targets, with the exception of the aC/Cu sample for 77 K. Presently we have no sound explanation for the yield difference observed for this measurement.

### E. Temperature dependence of the desorption yields

The results obtained from the above described heavy-ion-induced desorption measurements of cryogenic surfaces are summarized in Fig. 8, which also includes a comparison with earlier desorption yield measurements performed at CERN-LINAC 3 [5]. In this study we confirm that the heavy-ion-induced desorption yield is temperature
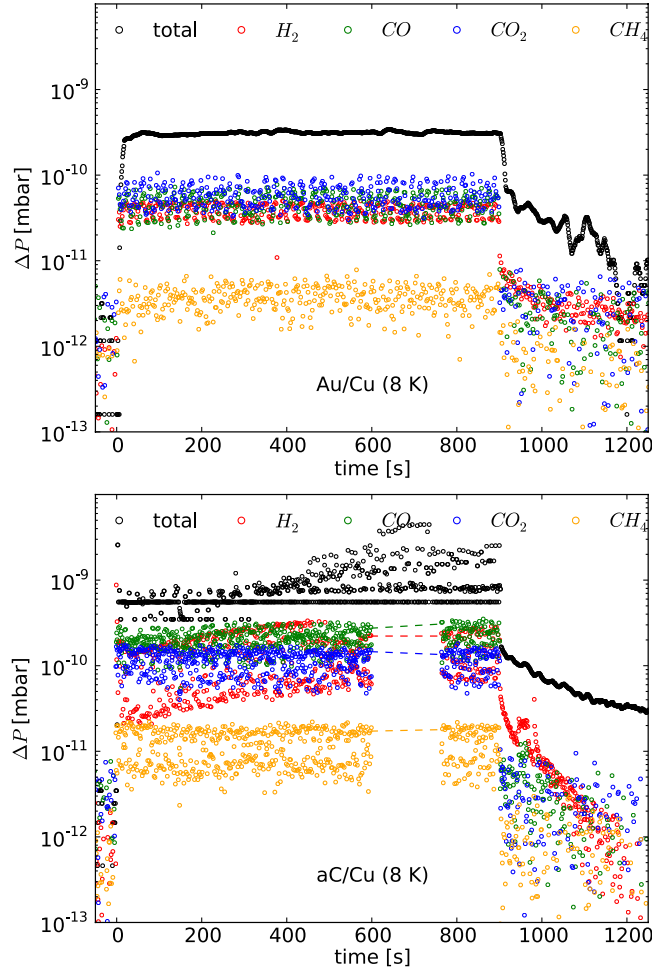
FIG. 7. Heavy-ion-induced pressure rises at 8 K target temperature. Partial pressure rises ($\Delta P$) of $H_2$, CO, $CO_2$, $CH_4$, and total pressure rises measured for the Au/Cu and aC/Cu samples continuously bombarded under $\theta = 0°$ with 1.4 MeV/u $Xe^{18+}$ ions are shown.

dependent; see Fig. 8 (left). For the amorphous-carbon-coated copper target, bombarded at GSI HLI under perpendicular impact with 1.4 MeV/u $Xe^{18+}$ ions, we measured a desorption yield of $\eta_{eff} \approx 1000$ molecules/ion at 8 K, which is a factor of $\approx 100$ lower compared with the 300 K value. Since for the gold-coated copper sample the yield reduction at 8 K is a factor of $\approx 12$, we find $\eta_{eff} \approx 430$ molecules/ion.

### 1. Comparison and discussion of results

In Fig. 8 (right) the HLI results of this study are compared with earlier LINAC 3 results. Both experiments had in common that all investigated targets were bombarded under perpendicular impact ($\theta = 0°$). The chosen target temperatures were nearly identical: 300 K, 77 K, 8 K (HLI), and 6.3 K (LINAC 3). In addition, both Au/Cu targets were fabricated from the same Cu raw material, cleaned, and finally gold coated at CERN using an

TABLE I. Heavy-ion-induced desorption yields calculated from the total and partial pressure rises for the Au/Cu sample, continuously bombarded under $\theta = 0°$ with 1.4 MeV/u $Xe^{18+}$ ions.

| Gas | $Xe^{18+}$(1.4 MeV/u) $\rightarrow$ Au/Cu | | |
|---|---|---|---|
| | $\eta_{eff}$(300 K) | $\eta_{eff}$(77 K) | $\eta_{eff}$(8 K) |
| $P_{tot}$ | 5500 | 620 | 430 |
| $H_2$ | 1100 | 560 | 230 |
| CO | 1500 | 150 | 98 |
| $CO_2$ | 840 | 150 | 120 |
| $CH_4$ | 140 | 16 | 15 |

TABLE II. Heavy-ion-induced desorption yields calculated from the total and partial pressure rises for the aC/Cu sample, continuously bombarded under $\theta = 0°$ with 1.4 MeV/u $Xe^{18+}$ ions.

| Gas | $Xe^{18+}$(1.4 MeV/u) $\rightarrow$ aC/Cu | | |
|---|---|---|---|
| | $\eta_{eff}$(300 K) | $\eta_{eff}$(77 K) | $\eta_{eff}$(8 K) |
| $P_{tot}$ | 129 000 | 3100 | 1000 |
| $H_2$ | 12 000 | 8400 | 1300 |
| CO | 53 000 | 210 | 400 |
| $CO_2$ | 43 000 | 180 | 170 |
| $CH_4$ | 3000 | 44 | 39 |

identical procedure. Significant differences between the HLI and LINAC 3 experiments are the projectile energies (1.4 MeV/u, 4.2 MeV/u) and the ion species ($Xe^{18+}$, $Pb^{54+}$). The experimental setups are also not identical but the measurement principle (pressure rise method) was the same.

We observe that the gold-coated copper targets have a similar desorption yield value at 300 K, i.e. 6200 molecules/$Pb^{54+}$ ion and 5400 molecules/$Xe^{18+}$ ion. Therefore, the yield measured with impacting $Xe^{18+}$ ions onto identically prepared targets is $\approx 12\%$ lower than the value obtained for $Pb^{54+}$. In previous studies [2,17] we found that the ambient temperature desorption yield is related to the electronic energy loss $(dE/dx)_{el}$ of the projectile as follows:

$$\eta = k \left( \frac{dE}{dx} \right)_{el}^n,$$

where $k$ is a scaling factor and $n$ can vary between 1.5 and 3. Calculating the electronic energy loss values for Pb (4.2 MeV/u) and Xe (1.4 MeV/u) ions using SRIM [18] and assuming $n = 2$, we obtain for $k = 1$ a value of $[(dE/dx)_{Xe}/(dE/dx)_{Pb}]^2 \approx 0.30$. This number compares with the experimentally found desorption yield ratio of $\approx 0.88$. Since the $k$ value is not known, we cannot explain the yield differences measured for the gold-coated copper
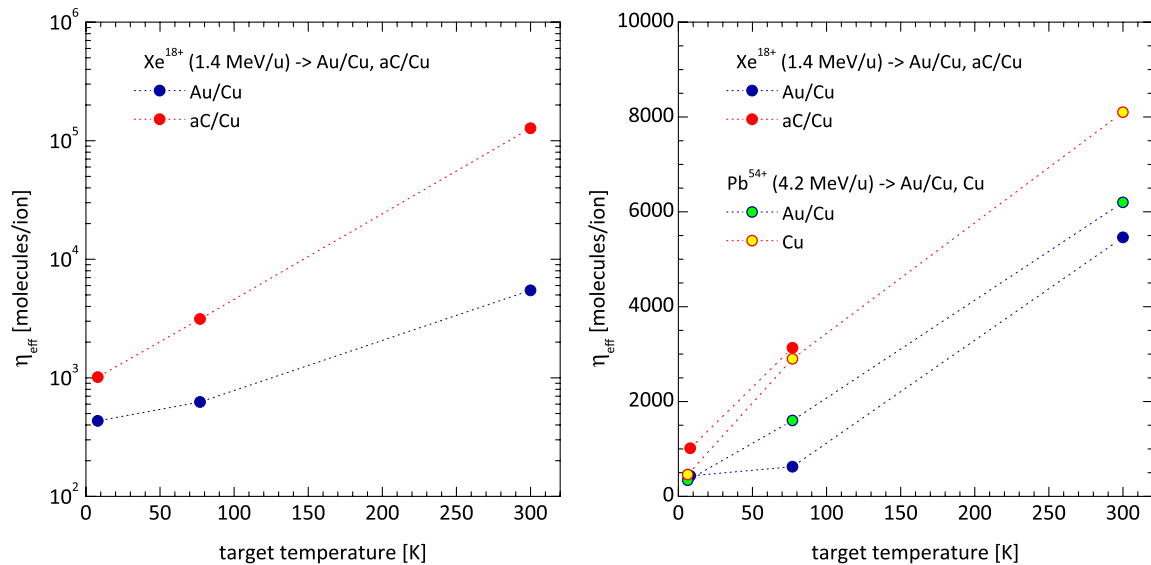
FIG. 8.    Left: temperature dependence of the heavy-ion-induced desorption yield of gold-coated and amorphous-carbon-coated copper surfaces bombarded under $\theta = 0°$ with 1.4 MeV/u Xe$^{18+}$ ions. Right: comparison of LINAC 3 desorption data obtained for 4.2 MeV/u Pb$^{54+}$ ions bombarding bare and gold-coated copper targets under $\theta = 0°$ [5].

targets. On the other hand, this discrepancy between the HLI and LINAC 3 desorption results is not surprising, since it is very well known that the amount of surface impurities, especially adsorbed carbon and oxygen, plays a significant role on the absolute values of $\eta_{eff}$ [11]. This argument may be supported by the different experimental conditions, e.g., the sample storage time in air and the bakeout temperature difference between the two experiments, which both can influence the amount of adsorbed carbon and oxygen on gold surfaces [7].

At 77 K the desorption yield difference for the two Au/Cu targets, bombarded with 1.4 MeV/u Xe$^{18+}$ ions and 4.2 MeV/u Pb$^{54+}$ ions, increases to $\approx 61\%$ (see Fig. 8). The observed yield difference between the two experiments may also be due to the amount of rest gas molecules adsorbed onto the target during the cool down from 300 to 77 K. Compared to the LINAC 3 experiment, the base pressure of the HLI setup, measured at ambient target temperature, was a factor of $\approx 12$ higher than at LINAC 3. We also have to mention the additional uncertainty due to the above described determination of the sticking coefficient.

For the HLI experiment at 8 K and the LINAC 3 experiment at 6.3 K, the heavy-ion-induced desorption rates of both gold-coated copper surfaces differ by $\approx 27\%$ [see Fig. 8 (right)]. It is interesting to note that for 3 out of 4 samples tested in two different experimental setups at GSI HLI and CERN LINAC 3, the heavy-ion-induced desorption yields of cryogenic targets, cooled down to the temperature range of about 6–8 K, are quite similar although the used projectile energies and charge states were significantly different. This holds for bare and

gold-coated copper, which have a yield of $\eta_{eff}$(6–8 K) $\approx$ 400 ± 60 molecules/ion. Only the copper target coated with amorphous carbon has a factor of $\approx 2.5$ higher desorption yield at 8 K.

### F. CO gas adsorption experiments at 8 K

The above described gas injection system, connected close to the samples placed in the experimental vacuum chamber, was used to inject CO gas onto the cryogenic target surfaces. The same experimental procedure as previously described in Ref. [5] was used in this study. CO gas was injected into the vacuum system, and a known amount of monolayers were adsorbed on the samples. In a second step, the gas was pumped out until the limit pressure of the system was reached again. Finally, each sample was continuously bombarded with 1.4 MeV/u Xe$^{18+}$ ions under perpendicular impact. The bombardment period was at least 5 min or until a stable pressure rise was obtained. Pressure data were taken continuously with the RGA and the extractor gauge. After the end of the ion bombardment, the vacuum system was pumped again until the limit pressure was obtained. Afterwards the same procedure was repeated with a higher number of adsorbed CO monolayers on the cryogenic surface. The results of these measurements, performed for the amorphous-carbon and gold-coated copper targets at 8 K are summarized in Fig. 9, which also includes a comparison with earlier gas adsorption measurements of the same type performed at CERN LINAC 3 [5].

The lowest desorption yields of $\eta_{eff} \approx$ 430 molecules/Xe$^{18+}$ ion (Au/Cu) and $\eta_{eff} \approx$ 520 molecules/Xe$^{18+}$ ion (aC/Cu) were measured at 8 K
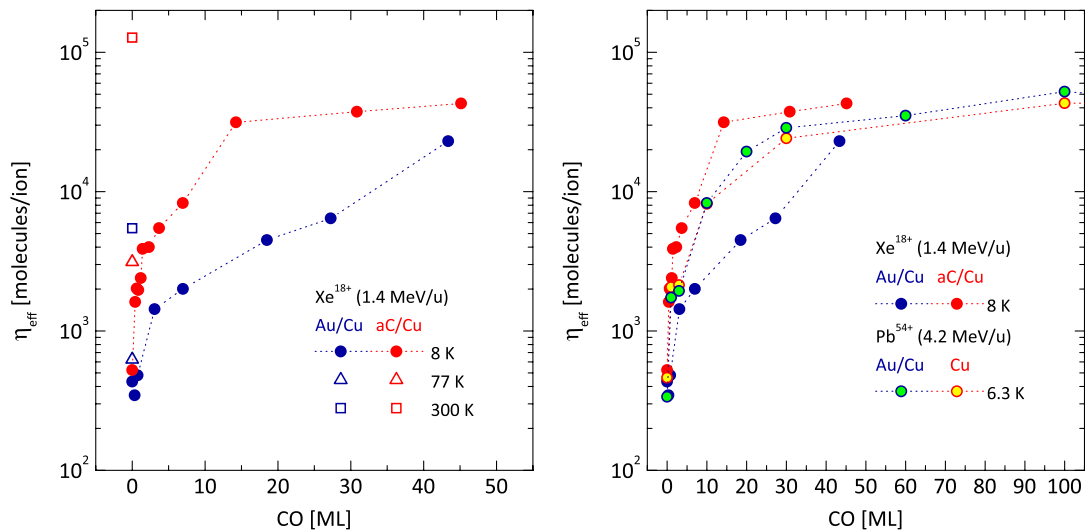
FIG. 9. Left: Heavy-ion-induced desorption yields as a function of adsorbed CO monolayers on gold-coated and amorphous-carbon-coated copper surfaces bombarded at 8 K with 1.4 MeV/u $Xe^{18+}$ ions under $\theta = 0°$. Right: comparison with LINAC 3 desorption data obtained for 4.2 MeV/u $Pb^{54+}$ ions bombarding under $\theta = 0°$ bare and gold-coated copper targets at 6.3 K [5].

without additional CO gas adsorption onto the cryogenic surfaces; see Fig. 9 (left). For the amorphous-carbon-coated target the 8 K desorption yield increases faster after the cryosorption of CO monolayers than the gold-coated target. After the adsorption of 1 ML of CO gas the yield increases by a factor of $\approx 4.2$ for carbon but remains nearly unchanged for the gold surface. The 77 K desorption yield value of both samples is reached with $\approx 1$–2 ML of CO gas adsorbed at 8 K. The ambient temperature desorption rate value of Au/Cu is exceeded after the cryosorption of more than $\approx 25$ ML of CO gas. With $\approx$ 45 ML, the heavy-ion-induced desorption yield is $\approx$ 43 000 molecules/ion for aC/Cu, still a factor of $\approx 3$ below the measured 300 K value. For both 8 K targets we find that with $\approx 45$ ML cryosorbed CO gas the heavy-ion-induced desorption yield is not yet constant; the effect is more pronounced for the gold-coated copper sample.

### 1. Comparison and discussion of results

In Fig. 9 (right) the above described HLI measurements are compared with earlier LINAC 3 results. It is remarkable that the bare and gold-coated copper targets, bombarded with 4.2 MeV/u $Pb^{54+}$ ions at LINAC 3, as well as the amorphous-carbon-coated copper target, bombarded with 1.4 MeV/u $Xe^{18+}$ ions at HLI, show the same desorption behavior at cryogenic temperature, i.e., the change in desorption yield as a function of cryosorbed CO monolayers is very similar for perpendicular heavy-ion impact. The LINAC 3 experiment has demonstrated that $\eta_{eff}$ continues to increase until 100 ML and remains constant up to 300 ML of cryosorbed CO gas. The gold-coated target, bombarded with $Xe^{18+}$ ions, shows a different behavior;

see Fig. 9 (right). At present we have no sound explanation for this difference.

### IV. SUMMARY AND CONCLUSION

Heavy-ion-induced desorption of gold-coated and amorphous-carbon-coated copper targets, bombarded at GSI HLI with 1.4 MeV/u $Xe^{18+}$ ions under $\theta = 0°$ perpendicular incidence, was studied at 300, 77, and 8 K. Desorption yields of $\eta_{eff}(8 \text{ K}) \approx 1000$ molecules/ion were measured for the carbon-coated and $\eta_{eff}(8 \text{ K}) \approx 430$ molecules/ion for the gold-coated copper target. These 8 K yields are a factor of $\approx 127$ (aC/Cu) and $\approx 13$ (Au/Cu) lower than the 300 K values. The low-temperature heavy-ion-induced desorption yields increased for both targets after a dedicated cryosorption of up to 45 monolayers of CO gas. A comparison with our previous LINAC 3 studies confirms qualitatively the correlation between $\eta_{eff}$ and the target temperature as well as the rise of $\eta_{eff}$ with adsorbed CO gas.

At present there is no reliable theory available that describes the heavy-ion-induced desorption phenomena and the measured desorption rates, neither for ambient nor for cryogenic target temperatures. Some progress has been recently made for desorption measurements with ambient temperature targets [19], but a deeper understanding of the underlying desorption mechanism is still lacking. Therefore, we suggest continuing the development of the inelastic thermal spike model and its extension to cryogenic target temperatures. We also want to highlight the practical impact of such a development, which would be very beneficial for the design, commissioning, and operation of future heavy-ion synchrotrons, for example, SIS100 of FAIR.

[1] E. Mahner, Phys. Rev. ST Accel. Beams **11**, 104801 (2008), and references therein.
[2] H. Kollmus, A. Krämer, M. Bender, M. C. Bellachioma, H. Reich-Sprenger, E. Mahner, E. Hedlund, L. Westerberg, O. B. Malyshev, M. Leandersson, and E. Edqvist, J. Vac. Sci. Technol. A **27**, 245 (2009).
[3] E. Hedlund, L. Westerberg, O. B. Malyshev, E. Edqvist, M. Leandersson, H. Kollmus, M. C. Bellachioma, M. Bender, A. Krämer, H. Reich-Sprenger, B. Zajec, and A. Krasnov, Nucl. Instrum. Methods Phys. Res., Sect. A **599**, 1 (2009).
[4] E. Mahner, M. Bender, and H. Kollmus, in *Proceedings of High Intensity and High Brightness Beams*, edited by I. Hofmann, J.-M. Lagniel, and R. W. Haase (Melville, New York, 2005), pp. 219–221; CERN Vacuum Technical Note 05-04, 2005.
[5] E. Mahner, L. Evans, D. Küchler, R. Scrivens, M. Bender, H. Kollmus, D. Severin, and M. Wengenroth, Phys. Rev. ST Accel. Beams **14**, 050102 (2011).
[6] "Facility for Antiproton and Ion Research in Europe GmbH," 2011, http://www.fair-center.de.
[7] E. Mahner, J. Hansen, D. Küchler, M. Malabaila, and M. Taborelli, Phys. Rev. ST Accel. Beams **8**, 053201 (2005).
[8] L. Bozyk, D. H. H. Hoffmann, P. Spiller, and H. Kollmus, in *Proceedings of the 2nd International Particle Accelerator Conference, San Sebastiàn, Spain* (EPS-AG, Spain, 2011), pp. 1527–1529.
[9] F. Caspers, G. Rumolo, W. Scandale, and F. Zimmermann, CERN Report No. CERN-BE-2009-005, 2008.
[10] C. Yin Vallgren, G. Arduini, J. Bauche, S. Calatroni, P. Chiggiato, K. Cornelis, P. Costa Pinto, B. Henrist, E. Mètral, H. Neupert, G. Rumolo, E. N. Shaposhnikova, and M. Taborelli, Phys. Rev. ST Accel. Beams **14**, 071001 (2011).
[11] E. Mahner, D. Holzer, D. Küchler, R. Scrivens, P. Costa Pinto, C. Yin Vallgren, and M. Bender, Phys. Rev. ST Accel. Beams **14**, 101001 (2011).
[12] K. Tinschert, D. M. Rueck, H. Emig, K. Leible, and N. Angert, Nucl. Instrum. Methods Phys. Res., Sect. B **113**, 59 (1996).
[13] P. Chiggiato and P. Costa Pinto, Thin Solid Films **515**, 382 (2006).
[14] E. Mahner, J. Hansen, J.-M. Laurent, and N. Madsen, Phys. Rev. ST Accel. Beams **6**, 013201 (2003).
[15] *Foundations of Vacuum Science and Technology*, edited by J. M. Lafferty (Wiley-Interscience, New York, 1998).
[16] R. Kersevan and J.-L. Pons, J. Vac. Sci. Technol. A **27**, 1017 (2009).
[17] A. W. Molvik, H. Kollmus, E. Mahner, M. K. Covo, M. C. Bellachioma, M. Bender, F. M. Bieniosek, E. Hedlund, A. Krämer, J. Kwan, O. B. Malyshev, L. Prost, P. A. Seidl, G. Westenskow, and L. Westerberg, Phys. Rev. Lett. **98**, 064801 (2007).
[18] J. F. Ziegler, M. D. Ziegler, and J. P. Biersack, Nucl. Instrum. Methods Phys. Res., Sect. B **268**, 1818 (2010).
[19] M. Bender, H. Kollmus, H. Reich-Sprenger, M. Toulemonde, and W. Assmann, Nucl. Instrum. Methods Phys. Res., Sect. B **267**, 885 (2009).